Quasi-orthogonal Space-frequency Coding in Non-coherent Cooperative Broadband Networks

Gbenga Owojaiye[1], Fabien Delestre[2] and Yichuang Sun[3]

School of Engineering and Technology

University of Hertfordshire

Hatfield, AL10 9AB United Kingdom

[1]g.owojaiye@herts.ac.uk [2]f.delestre@herts.ac.uk

[3]y.sun@herts.ac.uk

Abstract— **So far, complex valued orthogonal codes have been used differentially in cooperative broadband networks. These codes however achieve less than unitary code rate when utilized in cooperative networks with more than two relays. Therefore, the main challenge is how to construct unitary rate codes for non-coherent cooperative broadband networks with more than two relays while exploiting the achievable spatial and frequency diversity. In this paper, we extend full rate quasi-orthogonal codes to differential cooperative broadband networks where channel information is unavailable. From this, we propose a generalized differential distributed quasi-orthogonal space-frequency coding (DQSFC) scheme for cooperative broadband networks. Our proposed scheme is able to achieve full rate, and full spatial and frequency diversity in cooperative networks with any number of relays. Through pairwise error probability analysis we show that the diversity gain of our scheme can be improved by appropriate code construction and sub-carrier allocation. Based on this, we derive sufficient conditions for the proposed code structure at the source node and relay nodes to achieve full spatial and frequency diversity.**

Keywords—Differential distributed quasi-orthogonal space-frequency codes, orthogonal frequency division multiplexing, pairwise error probability, quasi-orthogonal codes

I. INTRODUCTION

The study of non-coherent signal detection in multiple-antenna broadband networks has been extensively investigated in the literature. For example in [1] [2] the authors investigate non-coherent maximum-likelihood (ML) detection of orthogonal space-time coded transmissions in ultra-wideband systems. Non-coherent signal detection in single-antenna cooperative networks has also become a popular research focus. The works in [3] [4] [5] propose differential transmission schemes for non-coherent signal

detection in quasi-static flat fading (narrowband) cooperative networks. The results show that different types of real and complex-valued codes can be used differentially in flat fading cooperative networks while guaranteeing full spatial and temporal diversity, and non-coherent detection. Compared to flat fading cooperative networks, the problem of non-coherent signal detection in frequency-selective fading (broadband) networks is significantly more challenging because of the presence of multiple channel paths and multiple broadcast phases between the source node and the destination. Furthermore, a simple extension of all the aforementioned non-coherent space-time coding schemes from the temporal dimension, to the frequency dimension, yields designs that are sub-optimal in terms of achievable frequency diversity. In other words, the direct application of codes in the temporal dimension to frequency sub-carriers fails to exploit the available diversity in the frequency dimension. Thus, while the schemes in [1-5] exploit achievable spatial and temporal gain, the schemes fail to exploit frequency diversity. The main problem is therefore how to design distributed space-frequency codes (DSFC) that can exploit the available diversity gain in the spatial and frequency dimensions in non-coherent broadband cooperative networks.

In addition to the aforementioned, the schemes in [1] [2] utilize orthogonal codes. It is difficult to construct orthogonal codes with full rate for cooperative networks with four or more relays. Quasi-orthogonal codes which achieve full rate have been studied in [6] for coherent flat fading networks where full channel state information (CSI) is available. For the case of non-coherent flat fading cooperative networks, quasi-orthogonal codes were employed in [7] for wireless relay networks with partial CSI. The results in [6] and [7] show that quasi-orthogonal codes can achieve full rate and full spatial and temporal diversity in flat fading channels. For the case of frequency-selective channels however, constructing quasi-orthogonal codes that can achieve full rate and full spatial and frequency diversity in non-coherent cooperative networks is more challenging and of practical requirement.

Motivated by all of the above, we propose a differential distributed quasi-orthogonal space-frequency coding (DQSFC) scheme which is able to achieve full rate, and full spatial and frequency diversity in non-coherent cooperative broadband networks with any number of relays. This means that our scheme achieves full rate when relay nodes forward information signals to the destination. We contrast our work with [8] and [9], while these works investigate hybrid combinations of quasi-orthogonal codes with

OFDM in coherent multiple-antenna networks. Our work is the first to focus on non-coherent single-antenna cooperative broadband networks utilizing quasi-orthogonal codes in the spatial and frequency dimensions. Based on all the aforementioned, in this work, we make the following contributions:

(1) As the cooperative network involves the 'transmit' and 'cooperate' stages, we carefully provide a systematic construction of the quasi-orthogonal space-frequency code matrix and present the full differential procedure. Based on the assumption of constant channel gain across adjacent groups of frequency sub-carriers, we implement the differential encoding, sub-carrier grouping and quasi-orthogonal design at the source node thereby simplifying the operation at the relays.

(2) The pairwise error probability (PEP) analysis shows that the diversity performance of our scheme can be improved through code construction and sub-carrier allocation. Based on this, we devise a code structure which maximizes the diversity performance of our scheme. Using the permutation scheme of [10], we introduce a sub-carrier allocation strategy which improves the diversity gain when CSI is unavailable.

(3) We study the performance of our proposed DQSFC scheme over frequency selective Rayleigh fading channels. From the simulation results, we show that the availability of different number of paths on the source-relay and relay-destination links provides additional diversity gains.

The rest of the paper is organized as follows: In Section II we present the quasi-orthogonal space frequency (QSF) system model and discuss how the space-frequency codes are designed at the source node and forwarded by the relays, we also present the structure of the quasi-orthogonal codes used in our scheme. Section III covers the encoding and decoding procedure for our differential DQSFC scheme. Section IV contains the PEP analysis and discussions on diversity improvement. Section V presents some simulation results and Section VI contains the conclusion.

Notation: A bold-face upper case letter denotes a matrix, while a bold-face lower case letter denotes a vector; $(\cdot)^*,(\cdot)^T,(\cdot)^H$ denote conjugate, transpose and conjugate-transpose respectively; $\boldsymbol{A}\odot\boldsymbol{B}$ denotes the Hadamard product or entry-wise product of the matrices $\boldsymbol{A}$ and $\boldsymbol{B}$; $\boldsymbol{A}\otimes\boldsymbol{B}$ denotes the Kronecker product of the matrices $\boldsymbol{A}$ and $\boldsymbol{B}$; $tr(\cdot)$ is a trace function; $E(\cdot)$ and $var(\cdot)$ represent expectation and variance of a random variable respectively; $\|\boldsymbol{X}\|_F$ denotes the Frobenius norm of the matrix $\boldsymbol{X}$; $|x|$ denotes the absolute value of x; $det(\boldsymbol{X})$ stands for the determinant of $\boldsymbol{X}$; $diag([x_0, x_1, \dots, x_{N-1}])$ denotes an $N \times N$

diagonal matrix with diagonal entries $x_0, x_1, \ldots, x_{N-1}$; $\lfloor x \rfloor$ denotes the largest integer smaller than x; $\boldsymbol{I}_N$ is an $N \times N$ identity matrix; superscript $\mathbb{C}^{T \times N}$ gives the dimension of a matrix of complex numbers; finally $j = \sqrt{-1}$.

II. DISTRIBUTED QUASI-ORTHOGONAL SPACE FREQUENCY CODING

A. System Model

The cooperative network consists of a source node, a destination node and P relay nodes as shown in Fig.1. Each node is equipped with a single antenna which is used for both transmission and reception. The transmission from the source node to the destination is divided into the 'transmit' and 'cooperate' stages. In the 'transmit' stage, the source node sends information signals to the cooperating relay nodes, while in the 'cooperate' stage, the source node keeps silent and the cooperating relay nodes simply forward the information signals to the destination. For each stage, the nodes are subject to half-duplex constraint such that they cannot transmit and receive simultaneously. We focus on differential DQSFC where the antennas of the cooperating nodes constructively forward the quasi-orthogonal codewords to the destination. We address the problem of differential encoding and decoding where the relay nodes and the destination are unable to acquire CSI. Our investigation in this work is carried out under the assumption of perfect inter-relay synchronization[1]. This assumption is however critical in practice due to the distributive nature of relays in space. Asynchronous transmission of the relays may result in degradation in diversity gain, specifically, the impact of synchronization errors have been studied in [11] based on analytical and simulation results.

The multipath fading channel between the source node and the p_{th} relay node is modeled as $f_p(t) = \sum_{l=0}^{L_{SR}-1} f_p(l)\delta(t-\alpha_l)$. Similarly, the multipath fading channel between the p_{th} relay node and the destination is modeled as $g_p(t) = \sum_{l=0}^{L_{RD}-1} g_p(l)\delta(t-\beta_l)$ where the complex amplitudes $f_p(l)$ and $g_p(l)$ are assumed to be independent zero-mean complex Gaussian random variables with variances $E\left(\left|f_p(l)\right|^2\right) = \sigma_{SR}^2(l)$ and $E\left(\left|g_p(l)\right|^2\right) = \sigma_{RD}^2(l)$ respectively. The delay of the l_{th} path is denoted by α_l and β_l, while $\delta(\cdot)$ is the Dirac delta function, L_{SR} and L_{RD} denote the number of independent channel taps on the source-relay $(S-R)$ link and relay-destination $(R-D)$ link

[1]It is noteworthy that the use of cyclic prefix can provide robustness against synchronization errors at the relays. This benefit, which is owed to the employment of OFDM transmission, is applicable to our proposed DQSFC scheme.

respectively. We assume that the channels are spatially uncorrelated, thus $f_p(l)$ and $g_p(l)$ are independent for different relay nodes. Unlike space-frequency coding in multiple-antenna systems, space-frequency coding in cooperative networks must be implemented in two distinct stages, namely; coding at the source node, and coding at the relay nodes. We first describe how the coded data is designed at the source node.

B. Source Node Coding

The cooperative system is based on OFDM modulation with N sub-carriers and T OFDM blocks. At the source node, a stream of N modulated symbols $\boldsymbol{s} = [s(0), s(1), \dots, s(N-1)]$ are generated from an $m = log_2 M$ $MPSK$ constellation, m is the spectral efficiency. The symbols are then encoded in such a way that a diversity of order $L = min\{L_{SR}, L_{RD}\}$ can be achieved at each relay node. In order to achieve this, we first define a fixed positive integer $\Gamma \leq L \ll N$, we then partition the N modulated symbols into $K = \lfloor N/P\Gamma \rceil$ blocks of codewords, such that each k_{th} block is of length $P\Gamma$. From this, we obtain the coded source node data

$$\boldsymbol{x} = [x(0), x(1), \dots, x(N-1)] = \left[\boldsymbol{x}_1^T, \boldsymbol{x}_2^T, \dots, \boldsymbol{x}_K^T, \boldsymbol{0}_{N-KP\Gamma}^T\right]^T \quad (1)$$

where $\boldsymbol{x}_k = [x_k(1), \dots, x_k(P\Gamma)]^T$ is the $P\Gamma \times 1$ coded source node data transmitted in the k_{th} block, $(N - KP\Gamma)$ zeros are padded into $\boldsymbol{x}$ if N is not an integer multiple of $P\Gamma$. The elements of $\boldsymbol{x}_k$ are stacked in parallel unto $P\Gamma$ adjacent data sub-carriers within a single OFDM block. We assume that the channel remains constant within each OFDM block, and varies independently from block to block. Based on this assumption, differentially modulated symbols will be placed on adjacent groups of $P\Gamma$ sub-carriers within the same OFDM block. Let $\boldsymbol{x}_k = [x_k(1), \dots, x_k(P\Gamma)]^T$ be the $P\Gamma \times 1$ data vector transmitted in the k_{th} block, where $x_k(n)$ denotes the symbol transmitted on the n_{th} sub-carrier. The elements of $\boldsymbol{x}$ are normalized such that $E(|\boldsymbol{x}_k|^2) = 1$. Since the source node transmits the data vector $\boldsymbol{x}_k$ to P relay nodes on $P\Gamma$ data sub-carriers, then the source node code is capable of achieving a diversity of order $\Gamma \leq L$ at each relay node. The criteria for achieving this diversity order will be clarified later.

If the data vector generated by the source node is of the form $\sqrt{E_S P\Gamma}\boldsymbol{x}_k$ where E_S denotes average transmit-power, the signal received at the p_{th} relay node in the k_{th} block after cyclic prefix[2] (CP) removal and fast Fourier transform (FFT) demodulation is given in vector form by:

$$\boldsymbol{r}_{k,p} = \sqrt{E_S P\Gamma}\boldsymbol{x}_k \odot \boldsymbol{f}_{k,p} + \boldsymbol{n}_{k,p} \tag{2}$$

where $\odot$ denotes Hadamard product or entry-wise operation, $\boldsymbol{r}_{k,p} = \left[r_{k,p}(1), \dots, r_{k,p}(P\Gamma)\right]^T$, $\boldsymbol{f}_{k,p} = \left[f_{k,p}(1), \dots, f_{k,p}(P\Gamma)\right]^T$ and $\boldsymbol{n}_{k,p} = \left[n_{k,p}(1), \dots, n_{k,p}(P\Gamma)\right]^T$ is the zero-mean complex Gaussian noise vector with covariance $N_0 I_{P\Gamma}$. The average signal-to-noise ratio (SNR) of the channel between the source node and the p_{th} relay node is given by $\Upsilon_{SR} = E_S P\Gamma / N_0$. The frequency response of the channel at the n_{th} sub-carrier of the p_{th} relay node in the k_{th} block is denoted by $f_{k,p}(n) = \sum_{l=0}^{L_{SR}-1} f_p(l) e^{-j2\pi ln/N} = \boldsymbol{f}_p \boldsymbol{\omega}, \boldsymbol{f}_p = \left[f_p(0), \dots, f_p(L_{SR}-1)\right], \boldsymbol{\omega} = \left[1, e^{-j2\pi n/N}, \dots, e^{-j2\pi L-1 n/N}\right]^T$.

C. Relay Node Coding

We now describe how the space-frequency codes are constructed at the relay nodes. Given that the p_{th} relay node receives $\boldsymbol{r}_{k,p}$ in (2) on $P\Gamma$ sub-carriers, it is only allowed to forward the data on Γ sub-carriers, while the data on the remaining $(P\Gamma - \Gamma)$ sub-carriers is discarded. Specifically, the p_{th} relay node is only allowed to forward a subset of $\boldsymbol{r}_{k,p}$ which we define as $\bar{\boldsymbol{r}}_{k,p} = \left[r_{k,p}(1), \dots, r_{k,p}(\Gamma)\right]^T \in \mathbb{C}^{\Gamma \times 1}$. Based on this, we can rewrite the received signal at the p_{th} relay node as:

$$\bar{\boldsymbol{r}}_{k,p} = \sqrt{E_S P\Gamma}\bar{\boldsymbol{x}}_k \odot \bar{\boldsymbol{f}}_{k,p} + \bar{\boldsymbol{n}}_{k,p} \tag{3}$$

where $\bar{\boldsymbol{x}}_k = [x_k(1), \dots, x_k(\Gamma)]^T$, $\bar{\boldsymbol{f}}_{k,p} = \left[f_{k,p}(1), \dots, f_{k,p}(\Gamma)\right]^T$ and $\bar{\boldsymbol{n}}_{k,p} = \left[n_{k,p}(1), \dots, n_{k,p}(\Gamma)\right]^T$. In our DQSFC scheme, the P relay nodes are designed to construct $\Gamma \times P$ quasi-orthogonal signal matrices at the destination. In order to achieve this, each p_{th} relay node is equipped with a $\Gamma \times \Gamma$ unitary matrix $\boldsymbol{M}_p$ referred to as the 'relay matrix'. The relay matrix is a matrix of 1s and 0s which enables the relay nodes to generate codewords with a quasi-orthogonal structure at the destination.The structure of the relay matrix is given in Section III and IV of [7] for cooperative networks with different number of relay nodes. Due to space limitations however, the structure of the relay matrix is not illustrated in our work, we simply

[2]The use of CP brings about additional bandwidth and power penalties due to the use of redundant symbols. Furthermore, the bandwidth and power losses are increased by a factor of P due to the multi-relay operation. Measures that can be used to reduce the inefficiency of the CP are documented in Chapter 4 of [12].

borrow the design of [7]. Specifically, we assume that J relay nodes are programmed to multiply their relay matrix by the received signal $\left[r_{k,p}(1),\dots,r_{k,p}(\Gamma)\right]^T$ while the remaining $P-J$ relay nodes are programmed to multiply their relay matrix by the conjugate of the received signal $\left[r_{k,p}(1)^*,\dots,r_{k,p}(\Gamma)^*\right]^T$. Thus, in the k_{th} block, the p_{th} relay node transmits a $\Gamma \times 1$ vector $\boldsymbol{t}_{k,p}$ given by:

$$\boldsymbol{t}_{k,p} = \sqrt{\frac{E_C}{E_S+1}}\boldsymbol{M}_p\bar{\boldsymbol{r}}_{k,p},\ \ \bar{\boldsymbol{r}}_{k,p} \in \left\{\left[r_{k,p}(1),\dots,r_{k,p}(\Gamma)\right]^T,\left[r_{k,p}(1)^*,\dots,r_{k,p}(\Gamma)^*\right]^T\right\} \tag{4}$$

The power allocated to each relay node is denoted by E_C, this implies that an amplification co-efficient $\mu = \sqrt{E_C/E_S+1}$ is applied at each relay node. The power allocation strategy is chosen to satisfy $E = \phi_1 E_S + \phi_2 E_C P$, we do not derive the optimal value for the power allocation factors ϕ_1 and ϕ_2 because exact channel knowledge is necessary to solve the optimization problem, and such optimization problem is outside the scope of this work. The interested reader is however referred to [13] where the issue of optimal power allocation for non-coherent cooperative networks is addressed explicitly.

Assuming the relay nodes are synchronized at symbol level such that the nodes can transmit simultaneously, the signal received at the destination in the k_{th} block after CP removal and FFT demodulation is given by:

$$\boldsymbol{y}_{k,n} = \sum_{p=1}^{P}\boldsymbol{t}_{k,p} \odot \boldsymbol{g}_{k,p} + \boldsymbol{z}_{k,n},\ \ n = 1,2,\dots,\Gamma \tag{5}$$

where $\boldsymbol{y}_{k,n} = \left[y_{k,n}(1),\dots,y_{k,n}(\Gamma)\right]^T$, $\boldsymbol{g}_{k,p} = \left[g_{k,p}(1),\dots,g_{k,p}(\Gamma)\right]^T$ and $\boldsymbol{z}_{k,n} = \left[z_{k,n}(1),\dots,z_{k,n}(\Gamma)\right]^T$ is the zero-mean complex Gaussian noise term with covariance $N_0 I_\Gamma$. The frequency response of the channel at the n_{th} sub-carrier between the p_{th} relay node and the destination in the k_{th} block is denoted by $g_{k,p}(n) = \sum_{l=0}^{L_{RD}-1} g_p(l)e^{-j2\pi ln/N} = \boldsymbol{g}_p\boldsymbol{\omega},\ \boldsymbol{g}_p = \left[g_p(0),\dots,g_p(L_{SR}-1)\right]$. The average SNR of the channel between the p_{th} relay node and the destination is given by $\Upsilon_{RD} = E_C/N_0$. Substituting for $\bar{\boldsymbol{r}}_{k,p}$ in (3) and $\boldsymbol{t}_{k,p}$ in (4), (5) becomes:

$$\boldsymbol{y}_{k,n} = \sum_{p=1}^{P}\sqrt{\frac{E_C E_S N_C}{E_S+1}}\boldsymbol{M}_p\bar{\boldsymbol{x}}_k \odot \bar{\boldsymbol{f}}_{k,p} \odot \boldsymbol{g}_{k,p} + \tilde{\boldsymbol{z}}_{k,n},\ \ n = 1,2,\dots,\Gamma \tag{6}$$

where $\tilde{\boldsymbol{z}}_{k,n} = \sum_{p=1}^{P}\mu\,\boldsymbol{M}_p\bar{\boldsymbol{n}}_{k,p} \odot \boldsymbol{g}_{k,p} + \boldsymbol{z}_{k,n}$ is the equivalent noise. The signal received at the destination in the k_{th} block can be written in compact form as:

$$\boldsymbol{Y}_k = \sqrt{\rho}\boldsymbol{X}_k\boldsymbol{H}_k + \boldsymbol{Z}_k \tag{7}$$

where $\boldsymbol{Y}_k = [\boldsymbol{y}_{k,1}, \dots, \boldsymbol{y}_{k,\Gamma}] \in \mathbb{C}^{\Gamma\times\Gamma}$, $\boldsymbol{y}_{k,n} = [y_{k,n}(1), \dots, y_{k,n}(\Gamma)]^T$, $\boldsymbol{X}_k = [\boldsymbol{M}_1\overline{\boldsymbol{x}}_k, \dots, \boldsymbol{M}_J\overline{\boldsymbol{x}}_k, \boldsymbol{M}_{J+1}\overline{\boldsymbol{x}}_k{}^*, \dots, \boldsymbol{M}_P\overline{\boldsymbol{x}}_k{}^*] \in \mathbb{C}^{\Gamma\times P}$, $\rho = \frac{E_C E_S N_C}{E_S+1}$, $\boldsymbol{H}_k = [\boldsymbol{h}_{k,1}, \dots, \boldsymbol{h}_{k,\Gamma}] \in \mathbb{C}^{P\times\Gamma}$, $\boldsymbol{h}_{k,n} = [h_k(1), \dots, h_k(P)]^T = (\boldsymbol{I}_P \otimes \boldsymbol{\omega}^T)\boldsymbol{h}$, $\boldsymbol{h} = [h_1(0), \dots, h_1(L-1), .., h_P(0), \dots, h_P(L-1)]^T$ and $\boldsymbol{Z}_k = [\tilde{\boldsymbol{z}}_{k,1}, \dots, \tilde{\boldsymbol{z}}_{k,\Gamma}] \in \mathbb{C}^{\Gamma\times\Gamma}$, the channel co-efficients $h_p(l) = f_p(l) \cdot g_p(l)$. The $P \times \Gamma$ quasi-orthogonal channel matrix $\boldsymbol{H}_k$ captures the channel co-efficients between the source node, the P relay nodes, and the destination. Here we assume that the channel is constant during the transmission of Γ symbols, that is, $\boldsymbol{h}_{k,n}$ is constant for $n = 1,2, \dots, \Gamma$.

The matrix $\boldsymbol{X}_k$ that is generated at the destination by the P relay nodes is a $\Gamma \times P$ quasi-orthogonal signal matrix containing either complex information symbols $\{x_k(1), \dots, x_k(\Gamma)\}$ or their conjugates $\{x_k(1)^*, \dots, x_k(\Gamma)^*\}$. Thus $\boldsymbol{X}_k$ in (7) can be rewritten as $\boldsymbol{X}_k = [\overline{\boldsymbol{x}}_{k,1}{}^T, \dots, \overline{\boldsymbol{x}}_{k,P}{}^T] \in \mathbb{C}^{\Gamma\times P}$, $\overline{\boldsymbol{x}}_{k,p} = [x_k(1), \dots, x_k(\Gamma)]$, where $\overline{\boldsymbol{x}}_{k,p}$ is the p_{th} column of $\boldsymbol{X}_k$. In other words, the p_{th} relay node transmits the p_{th} column vector of $\boldsymbol{X}_k$. In order to recover information symbols at the destination without CSI, two consecutive quasi-orthogonal signal matrices $\boldsymbol{X}_k$ and $\boldsymbol{X}_{k+1}$ must be received at the destination in the k_{th} block and $(k+1)_{th}$ block respectively. The first signal matrix $\boldsymbol{X}_k$ is termed the 'reference' quasi-orthogonal matrix because it is only required for differential decoding and thus contains no valid data, while the subsequent quasi-orthogonal signal matrix $\boldsymbol{X}_{k+1}$ conveys the valid data.

D. Quasi-Orthogonal Space-Frequency Code Construction

In this section, we devise the structure of QSF codes that can achieve our targeted diversity of order $P\Gamma$. Since quasi-orthogonal codes will be used to build the space-frequency codewords, it is necessary to employ the class of codes with a block-diagonal structure, for example, the quasi-orthogonal codes designed in [8] for multiple antenna systems. Denote $\boldsymbol{\mathcal{V}}$ as the generalized quasi-orthogonal matrix with a block-diagonal structure as given in [8], $\boldsymbol{\mathcal{V}}$ can be used to construct codewords for a cooperative network with any $P = 2q$ relay nodes where $q = 2^r$ for a positive integer r.

$$\boldsymbol{\mathcal{V}} = diag[\mathcal{G}(v_1, v_2), \mathcal{G}(v_3, v_4), \dots, \mathcal{G}(v_{P-1}, v_P) \dots], \mathcal{G}(v_i, v_j) = \begin{bmatrix} v_i & v_j \\ -v_j{}^* & v_i{}^* \end{bmatrix} \quad (8)$$

The entries of $\boldsymbol{\mathcal{V}}$ are made up of combined symbols, we now show how the combined symbols are computed. A stream of $m2\Gamma$ information bits are mapped into 2Γ symbols denoted by $\mathrm{v}_i, i = 1,2,\ldots,2\Gamma$. Using the design of [8], the symbols are combined as follows. Let $\Phi = \mathrm{D} \cdot diag\left[1, e^{j\theta_1}, \ldots, e^{j\theta_{\Gamma-1}}\right]$, where D is a $\Gamma \times \Gamma$ Hadamard matrix, the symbols are constructed as $[v_1, v_3, \ldots, v_{2\Gamma-1}]^T = \Phi \cdot [\mathrm{v}_1, \mathrm{v}_3, \ldots, \mathrm{v}_{2\Gamma-1}]^T$ and $[v_2, v_4, \ldots, v_{2\Gamma}]^T = \Phi \cdot [\mathrm{v}_2, \mathrm{v}_4, \ldots, \mathrm{v}_{2\Gamma}]^T$. Thus, the information symbols $\mathrm{v}_1, \mathrm{v}_2, \ldots, \mathrm{v}_{2\Gamma}$ are mapped onto different signal constellations due to the rotation angles θ, and the number of rotation angles depends on the size of the combined symbols. The rotation angles ensure that the codes achieve full diversity. As example, given a cooperative network with P relay nodes, the symbols are combined as $v_1 = \mathrm{v}_1 + \tilde{\mathrm{v}}_3 + \cdots + \mathrm{v}_{2\Gamma-1}, v_2 = \mathrm{v}_2 + \tilde{\mathrm{v}}_4 + \cdots + \mathrm{v}_{2\Gamma}$,…, $v_P = \mathrm{v}_1 - \tilde{\mathrm{v}}_3 - \cdots - \mathrm{v}_{2\Gamma-1}$ where $\tilde{\mathrm{v}}_i$ is the rotated version of v_i.

The main challenge is how to construct the source node codeword from $\boldsymbol{\mathcal{V}}$, such that spatial and frequency diversity is exploited, and full rate is guaranteed. For any cooperative network with P relay nodes, the quasi-orthogonal code for any k_{th} block $\boldsymbol{\mathcal{V}}_k$ is constructed from $\boldsymbol{\mathcal{V}}$ as

$$\boldsymbol{\mathcal{V}}_k = diag[\mathcal{G}(v_1, v_2), \ldots, \mathcal{G}(v_{P-1}, v_P)] \tag{9}$$

Using (9), the source node then constructs a $P \times 1$ codeword from the elements of $\boldsymbol{\mathcal{V}}_k$ as

$$\boldsymbol{v}_k = [v_1, \ldots, v_P]^T \tag{10}$$

The quasi-orthogonal code in (9) has full rate and will achieve full spatial diversity in any cooperative network with P relay nodes in a quasi-static flat fading channel scenario. The proof of full rate and full spatial diversity for the quasi-orthogonal code of (9) is given in [14, Section 5.4]. The code is however sub-optimal for our scheme because it is unable to exploit frequency diversity. In order to design a space-frequency codeword that guarantees full spatial and frequency diversity of order $P\Gamma$ where $\Gamma \leq L \ll N$, we follow the design of [8] and construct the quasi-orthogonal code from $\boldsymbol{\mathcal{V}}$ as

$$\boldsymbol{\mathcal{V}}_k = diag[\mathcal{G}(v_1, v_2), \ldots, \mathcal{G}(v_{P-1}, v_P), \ldots, \mathcal{G}(v_{P\Gamma-1}, v_{P\Gamma})] \tag{11}$$

Using (11), the source node then constructs a $P\Gamma \times 1$ codeword from the elements of $\boldsymbol{\mathcal{V}}_k$ as

$$\boldsymbol{v}_k = [v_1, \ldots, v_P, \ldots, v_{P\Gamma}]^T \tag{12}$$

The quasi-orthogonal code in (11) exploits full spatial and frequency diversity, the code also provides pairwise decoding as will be shown in Section III B. Note that $v_p,\ p \leq P$ in (12) are the original symbols, while $v_p,\ p > P$ are replicas of the original symbols which will be forwarded by the relay nodes.

As an example, for a cooperative network with $P = 4$ relay nodes, if we set $\Gamma = 4$, the $P\Gamma \times 1$ quasi-orthogonal source node data is constructed as

$$\boldsymbol{v}_k = \left[v_{i(1)}, \dots, v_{i(4)}, \dots, v_{i(16)}\right]^T, i \in \{1,2,..,\Gamma\}$$

$$= \left[\left(v_{1(1)}, v_{2(2)}, v_{3(3)}, v_{4(4)}\right), \left(v_{1(5)}, v_{2(6)}, v_{3(7)}, v_{4(8)}\right), \left(v_{1(9)}, v_{2(10)}, v_{3(11)}, v_{4(12)}\right),\right.$$

$$\left.\left(v_{1(13)}, v_{2(14)}, v_{3(15)}, v_{4(16)}\right)\right]^T$$

$$= [(v_1, v_2, v_3, v_4)_1, (-v_2{}^*, v_1{}^*, -v_4{}^*, v_3{}^*)_2, (-v_3{}^*, -v_4{}^*, v_1{}^*, v_2{}^*)_3, (v_4, -v_3, -v_2, v_1)_4]^T \quad (13)$$

where $v_{i(n)}, n \leq 4$ are the original information symbols and $v_{i(n)}, n > 4$ are replicas, $(\cdot)_p$ is the $\Gamma \times 1$ data vector that will eventually be forwarded by the p_{th} relay node during the 'cooperate' stage. Thus the proposed code structure guarantees full rate when the relay nodes transmit to the destination. Specifically, $v_1, \dots, v_\Gamma$ complex information symbols are transmitted simultaneously by P relay nodes on Γ sub-carriers. Our quasi-orthogonal code achieves a diversity order of $P\Gamma$ for any $(P + \Gamma) = 2^{r+1}, \forall\, P = \Gamma$ where r is a positive integer. In general, to construct the codeword for $(P + \Gamma) = J,\ 2^r < J < 2^{r+1}$, the quasi-orthogonal code is first constructed for $(P + \Gamma) = 2^{r+1}$ then $v_P,\ J < p \leq (P + \Gamma)$ is set to zero. For example, to obtain the codeword when $P = 4$ relay nodes and $\Gamma = 2$, that is $(P + \Gamma) = 6$, we first construct the codeword for $(P + \Gamma) = 2^{r+1} = 8$ then we set $\mathcal{G}(v_7, v_8)$ to zero.

III. DIFFERENTIAL ENCODING AND DECODING PROCEDURE

A. Differential Encoding Procedure

In this section, we discuss the differential encoding procedure employed in the proposed differential DQSFC scheme as depicted in Fig. 2. The architecture is typically composed of a hybrid combination of three functional sub-systems, namely, a constellation mapping sub-system, a differential sub-system and a space-frequency sub-system. Differential encoding is initiated at the source node. Recalling that $\boldsymbol{x}_k$ is the $P\Gamma \times 1$ coded source node data generated in the k_{th} block, the next step is for the source node to generate the $P\Gamma \times 1$ data $\boldsymbol{x}_{k+1}$ for the $(k + 1)_{th}$ block. This involves the following processes:

First, the constellation mapping sub-system generates the information symbols $\overline{\boldsymbol{v}}_{k+1} = [v_{k+1}(1), \dots, v_{k+1}(\Gamma)]^T$ where $\overline{\boldsymbol{v}}_{k+1}$ represents the combined symbol vector that must be recovered at the destination without CSI. Next, the differential encoder generates the $\Gamma \times 1$ data vector $\overline{\boldsymbol{x}}_{k+1} = [x_{k+1}(1), \dots, x_{k+1}(\Gamma)]^T$ for the $(k + 1)_{th}$ block as follows.

$$\bar{\boldsymbol{x}}_{k+1} = \boldsymbol{X}_k \bar{\boldsymbol{v}}_{k+1} \tag{14}$$

where $\boldsymbol{X}_k$ is the reference quasi-orthogonal signal matrix that was generated by the P relay nodes in the k_{th} block. We assume that the source node has prior knowledge of the relay matrices $\{\boldsymbol{M}_1, \dots, \boldsymbol{M}_J, \boldsymbol{M}_{J+1}, \dots, \boldsymbol{M}_P\}$, the source node also knows $\bar{\boldsymbol{x}}_k = [x_k(1), \dots, x_k(\Gamma)]^T$, hence it can compute $\boldsymbol{X}_k = \left[\boldsymbol{M}_1 \bar{\boldsymbol{x}}_k, \dots, \boldsymbol{M}_J \bar{\boldsymbol{x}}_k, \boldsymbol{M}_{J+1} \bar{\boldsymbol{x}}_k{}^*, \dots, \boldsymbol{M}_P \bar{\boldsymbol{x}}_k{}^*\right]$.

Then finally the source node constructs the $P\Gamma \times 1$ data $\boldsymbol{x}_{k+1} = [x_{k+1}(1), \dots, x_{k+1}(P\Gamma)]^T$ from $\bar{\boldsymbol{x}}_{k+1}$ by adding replicas as in (13). The quasi-orthogonal structure of $\bar{\boldsymbol{v}}_{k+1} \in \boldsymbol{\mathcal{V}}$ guarantees that $\bar{\boldsymbol{x}}_{k+1}$ is quasi-orthogonal.

The differential encoding process at the source node generates the $P\Gamma \times 1$ complex symbol vector $\boldsymbol{x}_{k+1} = [x_{k+1}(1), \dots, x_{k+1}(P\Gamma)]^T$ which is transmitted on $P\Gamma$ sub-carriers. In order to construct $\boldsymbol{X}_{k+1}$ at the destination, the source node and P relay nodes follow the same process as in the k_{th} block. The received signal at the p_{th} relay node in the $(k+1)_{th}$ block is of the form of (2). Similar to the case of the k_{th} block, the relay node data is constructed and transmitted as discussed in Section II C. The received signal at the destination in the $(k+1)_{th}$ block after FFT demodulation is similar to (7) and can be written in compact form as:

$$\boldsymbol{Y}_{k+1} = \sqrt{\rho} \boldsymbol{X}_{k+1} \boldsymbol{H}_{k+1} + \boldsymbol{Z}_{k+1} \tag{15}$$

B. Differential Decoding Procedure

As far as the destination is concerned, consecutive blocks of information codewords have been received across different sub-carriers. So far, consecutive quasi-orthogonal matrices $\boldsymbol{X}_k$ and $\boldsymbol{X}_{k+1}$ have been generated at the destination by P relay nodes based on (7) and (15). We can write

$$\boldsymbol{y}_{k,n} = \boldsymbol{X}_k \boldsymbol{h}_{k,n} + \tilde{\boldsymbol{z}}_{k,n} = \left[\bar{\boldsymbol{x}}_k{}^T \boldsymbol{H}_k + \tilde{\boldsymbol{z}}_{k,n}{}^T\right]^T, \; n = 1,2, \dots, \Gamma \tag{16}$$

$$\boldsymbol{y}_{k+1,n} = \boldsymbol{X}_{k+1} \boldsymbol{h}_{k+1,n} + \tilde{\boldsymbol{z}}_{k+1,n} = \left[\bar{\boldsymbol{x}}_{k+1}{}^T \boldsymbol{H}_{k+1} + \tilde{\boldsymbol{z}}_{k+1,n}{}^T\right]^T \; n = 1,2, \dots, \Gamma \tag{17}$$

Note that we intentionally omit the power term $\sqrt{\rho}$ for ease of explanation. Using the signals received in (16) and (17) in the k_{th} block and $(k+1)_{th}$ block respectively, $\bar{\boldsymbol{v}}_{k+1} = [v_{k+1}(1), \dots, v_{k+1}(\Gamma)]^T$ can be recovered pairwisely at the destination without CSI. For example, for a cooperative network with $P = 4$ relay nodes and $\Gamma = 4$, in order to recover $\bar{\boldsymbol{v}}_{k+1}$ we first obtain the quasi-orthogonal signal and channel matrices for two consecutive transmission blocks as follows:

$$\boldsymbol{X}_j = \begin{bmatrix} x_j(1) & x_j(2) & x_j(3) & x_j(4) \\ -x_j(2)^* & x_j(1)^* & -x_j(4)^* & x_j(3)^* \\ -x_j(3)^* & -x_j(4)^* & x_j(1)^* & x_j(2)^* \\ x_j(4) & -x_j(3) & -x_j(2) & x_j(1) \end{bmatrix}, \boldsymbol{H}_j = \begin{bmatrix} h_j(1) & h_j(2)^* & h_j(3)^* & h_j(4) \\ h_j(2) & -h_j(1)^* & h_j(4)^* & -h_j(3) \\ h_j(3) & h_j(4)^* & -h_j(1)^* & -h_j(2) \\ h_j(4) & -h_j(3)^* & -h_j(2)^* & h_j(1) \end{bmatrix}$$

where $\boldsymbol{X}_j$ and $\boldsymbol{H}_j$, $j \in \{k, k+1\}$ are quasi-orthogonal signal and channel matrices respectively. The information signal transmitted by the source node, through the p_{th} relay node on the n_{th} subcarrier is denoted by $x_j(n)$, and $h_j(p)$ captures the channel co-efficients between the source node, the p_{th} relay node, and the destination. Based on this, we can compute

$$\boldsymbol{X}_j \boldsymbol{X}_j{}^H = \begin{bmatrix} X_1 & 0 & 0 & X_2 \\ 0 & X_1 & -X_2 & 0 \\ 0 & -X_2 & X_1 & 0 \\ X_2 & 0 & 0 & X_1 \end{bmatrix} \boldsymbol{H}_j \boldsymbol{H}_j{}^H = \begin{bmatrix} H_1 & 0 & 0 & H_2 \\ 0 & H_1 & -H_2 & 0 \\ 0 & -H_2 & H_1 & 0 \\ H_2 & 0 & 0 & H_1 \end{bmatrix}$$

where $X_1 = \sum_{n=1}^{4} \left| x_j(n) \right|^2$ is the signal power and $X_2 = 2Re\left(x_j(1)x_j(4)^* - x_j(2)x_j(3)^* \right)$ is a self-interference parameter. Similarly, $H_1 = \sum_{p=1}^{4} \left| h_j(p) \right|^2$ is the channel power and $H_2 = 2Re\left\{ h_j(1)h_j(4)^* - h_j(2)h_j(3)^* \right\}$ is a self-interference parameter. The elements of $\overline{\boldsymbol{v}}_{k+1}$ are then recovered as follows:

$$\boldsymbol{y}_{k+1,1}\, \boldsymbol{y}_{k,1}{}^H = \overline{\boldsymbol{x}}_{k+1} \boldsymbol{X}_k{}^H \boldsymbol{H}_{k+1} \boldsymbol{h}_{k,1}{}^H + Z_1 = \overline{\boldsymbol{v}}_{k+1} \boldsymbol{X}_k \boldsymbol{X}_k{}^H \boldsymbol{H}_{k+1} \boldsymbol{h}_{k,1}{}^H + Z_1$$

$$= v_{k+1}(1)(X_1H_1 + X_2H_2) + v_{k+1}(4)(X_1H_2 + X_2H_1) + Z_1 = v_{k+1}(1)A + v_{k+1}(4)B + Z_1 \quad (18)$$

Similarly,

$$\boldsymbol{y}_{k+1,1}\, \boldsymbol{y}_{k,2}{}^H = \overline{\boldsymbol{x}}_{k+1} \boldsymbol{X}_k{}^H \boldsymbol{H}_{k+1} \boldsymbol{h}_{k,2}{}^H + Z_2 = v_{k+1}(2)A - v_{k+1}(3)B + Z_2 \quad (19)$$

$$\boldsymbol{y}_{k+1,1}\, \boldsymbol{y}_{k,3}{}^H = \overline{\boldsymbol{x}}_{k+1} \boldsymbol{X}_k{}^H \boldsymbol{H}_{k+1} \boldsymbol{h}_{k,3}{}^H + Z_3 \; = -v_{k+1}(2)B + v_{k+1}(3)A + Z_3 \quad (20)$$

$$\boldsymbol{y}_{k+1,1}\, \boldsymbol{y}_{k,4}{}^H = \overline{\boldsymbol{x}}_{k+1} \boldsymbol{X}_k{}^H \boldsymbol{H}_{k+1} \boldsymbol{h}_{k,4}{}^H + Z_4 \; = v_{k+1}(1)B + v_{k+1}(4)A + Z_4 \quad (21)$$

where Z_n captures the noise, $A = X_1H_1 + X_2H_2$ and $B = X_1H_2 + X_2H_1$, we refer to A and B as the differential decoding parameters required to recover $\overline{\boldsymbol{v}}_{k+1}$. The differential decoding parameters are computed at the destination as:

$$\boldsymbol{y}_{k,1}\, \boldsymbol{y}_{k,4}{}^H = \boldsymbol{X}_k \boldsymbol{h}_{k,1} \boldsymbol{X}_k{}^H \boldsymbol{h}_{k,4}{}^H + \tilde{Z}_4 = A + \tilde{Z}_4$$

$$\boldsymbol{y}_{k,1}\, \boldsymbol{y}_{k,1}{}^H = \boldsymbol{X}_k \boldsymbol{h}_{k,1} \boldsymbol{X}_k{}^H \boldsymbol{h}_{k,1}{}^H + \tilde{Z}_1 = B + \tilde{Z}_1 \quad (22)$$

This implies that $\boldsymbol{y}_{k,1}\,\boldsymbol{y}_{k,4}{}^{H} \approx A$ and $\boldsymbol{y}_{k,1}\,\boldsymbol{y}_{k,1}{}^{H} \approx B$ since $Z_n \approx \tilde{Z}_n$. It is thus obvious from (22) that the scheme does not require CSI to recover $\overline{\boldsymbol{v}}_{k+1}$. The non-coherent recovery of $\overline{\boldsymbol{v}}_{k+1}$ rather depends on consecutively received signals in the k_{th} block and $(k+1)_{th}$ block under the constraint that $\boldsymbol{H}_k \cong \boldsymbol{H}_{k+1}$. Once A and B are computed at the destination using (22), the information signals in (18) to (21) can be recovered pairwisely. The decoding complexity of our space-frequency codeword is exponential in Γ. It is thus necessary to set Γ such that a trade-off is reached between decoding complexity and frequency diversity. If we choose $1 \le \Gamma \le L$, then our scheme provides enough flexibility such that the necessary trade-off is achieved for any design preference.

IV. Pairwise Error Probability Analysis and Diversity Improvement

A. Pairwise Error Probability Analysis

We now proceed to develop sufficient design criteria, based on the PEP analysis, for our code to achieve full diversity of order $P\Gamma$ while the coding gain is maximized as much as possible. Since each of the K blocks contains arbitrary symbols which are independently distributed across the relay nodes, we only require a single block k for our PEP analysis, which is valid for any $k = 1,2,\dots,K$. The frequency response vector between the source node and the relay nodes is denoted by $\boldsymbol{f}_k = [f_k(1),\dots,f_k(P\Gamma)]^T$, and similarly, the frequency response vector between the relay nodes and the destination is $\boldsymbol{g}_k = \left[g_{k,1}(1),\dots,g_{k,1}(\Gamma),\dots,g_{k,P}(1),\dots,g_{k,P}(\Gamma)\right]^T$. The correlation matrix of the channel frequency response can be found as $\boldsymbol{R} = E\{\boldsymbol{h}_k\boldsymbol{h}_k{}^{H}\} = E\{(\boldsymbol{f}_k \odot \boldsymbol{g}_k)(\boldsymbol{f}_k \odot \boldsymbol{g}_k)^H\}$. Unlike the case of multiple antenna systems, the cooperative network has the 'transmit' and 'cooperate' stages, thus $\boldsymbol{R}$ can be decomposed as $\boldsymbol{R} = \boldsymbol{R}_1 \odot \boldsymbol{R}_2$. We can easily show that $\boldsymbol{R}$, $\boldsymbol{R}_1$ and $\boldsymbol{R}_2$ are full rank based on the following:

$$\boldsymbol{R}_1 = E\{\boldsymbol{f}_k\boldsymbol{f}_k{}^{H}\} = \boldsymbol{W}_1 E\{\boldsymbol{f}_p\boldsymbol{f}_p{}^{H}\}\boldsymbol{W}_1{}^{H}$$

$$= \boldsymbol{W}_1 diag(\sigma_{SR}{}^2(0),\dots,\sigma_{SR}{}^2(L_{SR}-1))\boldsymbol{W}_1{}^{H} \quad (23)$$

$$\boldsymbol{R}_2 = E\{\boldsymbol{g}_k\boldsymbol{g}_k{}^{H}\} = \boldsymbol{W}_2 E\{\boldsymbol{g}_p\boldsymbol{g}_p{}^{H}\}\boldsymbol{W}_2{}^{H}$$

$$= \boldsymbol{W}_2 diag(\sigma_{RD}{}^2(0),\dots,\sigma_{RD}{}^2(L_{RD}-1))\boldsymbol{W}_2{}^{H} \quad (24)$$

$$\boldsymbol{W}_1 = \left[\boldsymbol{w}^{\alpha_0{}^T},\dots,\boldsymbol{w}^{\alpha_{L-1}{}^T}\right], \boldsymbol{W}_2 = \left[\boldsymbol{w}^{\beta_0{}^T},\dots,\boldsymbol{w}^{\beta_{L-1}{}^T}\right], \boldsymbol{w} = \left[1,\omega^1,\dots,\omega^{(P\Gamma-1)}\right], \omega = e^{-j2\pi\Delta f} \quad (25)$$

where $\boldsymbol{f}_p = \left[f_p(0), \dots, f_p(L_{SR}-1)\right]^T$ and $\boldsymbol{g}_p = \left[g_p(0), \dots, g_p(L_{RD}-1)\right]^T$ and $\Delta f = 1/T$ is the sub-carrier spacing. From (25) if $\boldsymbol{W}_1$ and $\boldsymbol{W}_2$ are unitary matrices[3], (valid if all L_{SR} and L_{RD} fall within the sampling instances of the relay nodes and destination respectively [15][16]) then $\boldsymbol{W}_1$ and $\boldsymbol{W}_2$ have full rank, $R_{\boldsymbol{W}_1} = \Gamma \leq L$ and $R_{\boldsymbol{W}_2} = \Gamma \leq L$, respectively. We can then verify that $\boldsymbol{R}$, $\boldsymbol{R}_1$ and $\boldsymbol{R}_2$ are positive definite (full rank correlation matrices) based on the theorem in Section 1.2.4 of [17], which states that; if $\boldsymbol{R}_1$ and $\boldsymbol{R}_2$ are positive definite, then $\boldsymbol{R}$ is itself a positive definite (full rank correlation matrix).

Since we have established that $\boldsymbol{R}$ has full rank, we now proceed to discuss the criteria to achieve maximum diversity. We define statistically independent samples of the $S-R$ channel as $\boldsymbol{f} = [f_1(0), \dots, f_1(L_{SR}-1), \dots, f_P(0), \dots, f_P(L_{SR}-1)]$. Similarly, statistically independent samples of the $R-D$ channel are defined as $\boldsymbol{g} = [g_1(0), \dots, g_1(L_{RD}-1), \dots, g_P(0), \dots, g_P(L_{RD}-1)]$. Under the assumption that all $f_p(l)$and $g_p(l)$ are independent identically distributed complex Gaussian variables, we can imply that $\boldsymbol{h} = [h_1(0), \dots, h_1(L-1), \dots, h_P(0), \dots, h_P(L-1)]$, $h_p(l) = f_p(l) \cdot g_p(l)$. For any k_{th} block, the SF codeword can be viewed as a collection of symbols transmitted across Γ sub-carriers by P relay nodes. Based on this, the consecutively received signals at the destination in the k_{th} block and $(k+1)_{th}$ block can be rewritten as (26) under the constraint that the sub-channel gain of adjacent blocks of sub-carriers is almost constant.

$$\boldsymbol{Y}^k = \overline{\boldsymbol{X}}^k \boldsymbol{\Lambda} \boldsymbol{h} + \boldsymbol{Z}^k$$

$$\boldsymbol{Y}^{k+1} = \overline{\boldsymbol{X}}^{k+1} \boldsymbol{\Lambda} \boldsymbol{h} + \boldsymbol{Z}^{k+1} \tag{26}$$

where $\boldsymbol{Y}^k = \left[\boldsymbol{y}_1^k, \dots, \boldsymbol{y}_\Gamma^k\right]^T$, $\boldsymbol{y}_n^k = [y^k(1), \dots, y^k(\Gamma)]^T$,$\boldsymbol{Y}^{k+1} = \left[\boldsymbol{y}_1^{k+1}, \dots, \boldsymbol{y}_\Gamma^{k+1}\right]^T$,$\boldsymbol{y}_n^{k+1} = [y^{k+1}(1), \dots, y^{k+1}(\Gamma)]^T$, $\overline{\boldsymbol{X}}^k = diag\left[\boldsymbol{x}_{k,1}, \dots, \boldsymbol{x}_{k,\Gamma}\right]$,$\boldsymbol{x}_{k,n} = \left[x_{k,n}(1), \dots, x_{k,n}(P)\right]$,$\overline{\boldsymbol{X}}^{k+1} = diag\left[\boldsymbol{x}_{k+1,1}, \dots, \boldsymbol{x}_{k+1,\Gamma}\right]$,$\boldsymbol{x}_{k+1,n} = \left[x_{k+1,n}(1), \dots, x_{k+1,n}(P)\right]$, $\boldsymbol{\Lambda} = [\boldsymbol{\Lambda}(1), \dots, \boldsymbol{\Lambda}(\Gamma)]^T$,$\boldsymbol{\Lambda}(n) = \boldsymbol{I}_P \otimes \boldsymbol{\omega}^T$, $\boldsymbol{\omega} = \left[1, e^{-j2\pi n/N}, \dots, e^{-j2\pi L-1 n/N}\right]^T$.

Using the following notations:

$\boldsymbol{Y} = \left[\boldsymbol{Y}^{k^T}, \boldsymbol{Y}^{k+1^T}\right]^T$, $\boldsymbol{V}^{k+1} = diag\left[\boldsymbol{v}_{k+1,1}, \dots, \boldsymbol{v}_{k+1,\Gamma}\right]$, $\boldsymbol{v}_{k+1,n} = \left[v_{k+1,n}(1), \dots, v_{k+1,n}(P)\right]$, $\boldsymbol{X} = \left[\boldsymbol{I}_{\mathrm{P}\Gamma}{}^T, \boldsymbol{V}^{k+1^T}\right]$, $\boldsymbol{Z} = \left[\boldsymbol{Z}^{k^T}, \boldsymbol{Z}^{k+1^T}\right]^T$, and the recursion

[3]Generally in OFDM systems, the FFT process causes correlation among the frequency sub-carriers. Based on the assumption that the FFT matrix is unitary and all the path delays fall within the sampling instances of the receiver, then $\boldsymbol{W}_1$ and $\boldsymbol{W}_2$ which are part of the FFT matrix, are unitary matrices.

$$\bar{\boldsymbol{X}}^{k+1} = \begin{cases} \boldsymbol{V}^{k+1}\bar{\boldsymbol{X}}^{k}, & k \geq 1 \\ \boldsymbol{I}_{P\Gamma}, & k = 0 \end{cases}.$$

we can show that the performance of our code is determined by $\boldsymbol{R}$, $\boldsymbol{\Lambda}^H\boldsymbol{\Lambda}$ and $\left(\acute{\boldsymbol{V}}^{k+1} - \boldsymbol{V}^{k+1}\right)^H\left(\acute{\boldsymbol{V}}^{k+1} - \boldsymbol{V}^{k+1}\right)$, the derivations leading to this deduction is given in Appendix A. We have already established that $\boldsymbol{R}$ has full rank, thus our scheme will achieve maximum diversity if and only if $\boldsymbol{\Lambda}^H\boldsymbol{\Lambda}$ and $\left(\acute{\boldsymbol{V}}^{k+1} - \boldsymbol{V}^{k+1}\right)^H\left(\acute{\boldsymbol{V}}^{k+1} - \boldsymbol{V}^{k+1}\right)$ have full rank. Since we are interested in achieving maximum diversity while the coding gain is maximized as much as possible, the code must be designed such that $\acute{\boldsymbol{V}}^{k+1} - \boldsymbol{V}^{k+1}$ has full rank PL over all possible pairwise errors. When maximum diversity is achieved, that is when $\acute{\boldsymbol{V}}^{k+1} - \boldsymbol{V}^{k+1}$ has full rank, the coding gain is only determined by $\det(\boldsymbol{\Lambda}^H\boldsymbol{\Lambda})$ and $\det\left[\left(\acute{\boldsymbol{V}}^{k+1} - \boldsymbol{V}^{k+1}\right)^H\left(\acute{\boldsymbol{V}}^{k+1} - \boldsymbol{V}^{k+1}\right)\right]$. In order to maximize the coding gain, the first step is to provide PL uncorrelated channels such that $\det(\boldsymbol{\Lambda}^H\boldsymbol{\Lambda})$ is maximized. For the second step, we consider the diversity product ζ_c which measures the quality of the code given as $\zeta_c = \frac{1}{2}\min_{\acute{\boldsymbol{V}}^{k+1} \neq \boldsymbol{V}^{k+1} \forall \boldsymbol{\mathcal{V}}} \left|\det\left(\acute{\boldsymbol{V}}^{k+1} - \boldsymbol{V}^{k+1}\right)\right|^{\frac{1}{PL}}$ where $\zeta_c > 0$ achieves maximum diversity. Thus the coding gain is maximized when we maximize ζ_c under the constraint that: $0 \leq \zeta_c \leq 1$ and $\left(\acute{\boldsymbol{V}}^{k+1} - \boldsymbol{V}^{k+1}\right), \forall\, \acute{\boldsymbol{V}}^{k+1} \neq \boldsymbol{V}^{k+1}$. Next we discuss the measures taken to maximize ζ_c based on code construction and to maximize $\det(\boldsymbol{\Lambda}^H\boldsymbol{\Lambda})$ based on sub-carrier grouping.

B. Diversity Improvement Based on Code Design

We now discuss the criteria for our block-diagonal quasi-orthogonal code $\boldsymbol{\mathcal{V}}_k, k = 1,2,\ldots,K$ of (11) to achieve full diversity. When SNR is high and when the relay nodes and destination are unable to acquire CSI, we have identified that the performance of our code is determined by the diversity product ζ_c which is given in the previous section. Hence our focus is to build constellations that maximize ζ_c as much as possible. As a first step, we prove that our code satisfies the full diversity criterion for space-frequency codes given in Theorem 3.1 of [10], the proof is provided in Appendix B. Based on this, we can calculate the overall diversity product

$$\zeta_{eq} = \frac{1}{2}\min_{\forall \acute{\boldsymbol{v}}_k \neq \boldsymbol{v}_k \in \boldsymbol{\mathcal{V}}} \left|det\left(\left[\left(\boldsymbol{\mathcal{V}}_k - \acute{\boldsymbol{\mathcal{V}}}_k\right)^H\left(\boldsymbol{\mathcal{V}}_k - \acute{\boldsymbol{\mathcal{V}}}_k\right)\right] \odot \boldsymbol{R}\right)\right|^{\frac{1}{2P\Gamma}}$$

$$= \frac{1}{2}\min_{\forall \acute{v}_k \neq \boldsymbol{v}_k \in \boldsymbol{\mathcal{V}}} \prod_{p=1}^{P\Gamma} \left|v_p - \acute{v}_p\right|^{\frac{1}{P\Gamma}} \left|\det(\boldsymbol{R})\right|^{\frac{1}{2\Gamma}}$$

$$= \frac{1}{2} \min_{\forall \acute{\boldsymbol{V}}^{k+1} \neq \boldsymbol{V}^{k+1} \in \boldsymbol{\mathcal{V}}} \left|\det\left(\acute{\boldsymbol{V}}^{k+1} - \boldsymbol{V}^{k+1}\right)\right|^{\frac{1}{P\Gamma}} |\det(\boldsymbol{R})|^{\frac{1}{2\Gamma}} = \zeta_c . |\det(\boldsymbol{R})|^{\frac{1}{2\Gamma}} \quad (27)$$

where $\boldsymbol{\mathcal{V}}_k$ and $\acute{\boldsymbol{\mathcal{V}}}_k$ are two distinct pair of codewords. From (27) we can observe that if our code is constructed such that $\prod_{p=1}^{P\Gamma} \left|v_p - \acute{v}_p\right|^2 \neq 0$, then ζ_{eq} is non-zero and our scheme achieves diversity order of $P\Gamma, \Gamma \leq L$. Thus $|\det(\boldsymbol{R})|^{\frac{1}{2L}}$ which is determined by the power profile of the channel, $\sigma(l) = \sigma_{SR}(l) \cdot \sigma_{RD}(l)$, is independent of the code structure. Likewise ζ_c which is independent of the power profile, is only dependent on the constellation design and code structure which are optimized for maximum ζ_c.

C. Diversity Improvement based on Sub-carrier Interleaving

In order to improve the diversity product, an appropriate sub-carrier allocation method which maximizes $\det(\boldsymbol{\Lambda}^H \boldsymbol{\Lambda})$ must be selected. The distribution of K codewords across $P\Gamma$ equally spaced blocks of sub-carriers as implemented in our system model has been shown to maximize $\det(\boldsymbol{\Lambda}^H \boldsymbol{\Lambda})$ in [18]. This is subject to the assumption that $\boldsymbol{\Lambda}$ is unitary. To further improve the coding gain of the DQSFC scheme we introduce a sub-carrier allocation method based on the permutation scheme of [10] which requires prior knowledge of the channel. However, if the source node and the relay nodes lack prior knowledge of the power delay profile (${\sigma_{SR}}^2$, ${\sigma_{RD}}^2$, α_l and β_l) of the channels, a randomized interleaving scheme can be utilized [10].

The elements of the quasi-orthogonal codeword $\boldsymbol{v}_k = [v_1, \dots, v_P, \dots, v_{P\Gamma}]^T, k = 1,2, \dots, K$ of (12) are re-allocated to a new set of sub-carriers such that we obtain the interleaved version of $\boldsymbol{v}_k$ which is given by $\varrho(\boldsymbol{v}_k)$. Given the difference operation $(\boldsymbol{v}_k - \acute{\boldsymbol{v}}_k), \forall \acute{\boldsymbol{v}}_k \neq \boldsymbol{v}_k$, we can equivalently write $\left(v_p - \acute{v}_p\right), \forall \acute{v}_p \neq v_p$, where $p = 1,2, \dots, P\Gamma$. Based on the sub-carrier allocation method, $\left(v_p - \acute{v}_p\right)$ is now set as the $n_p th$ entry of $\varrho\{(\boldsymbol{v} - \acute{\boldsymbol{v}})\}$, or in simpler terms, v_p which was initially transmitted on the n_{th} sub-carrier is now transmitted on the $n_p th$ $\left(0 \leq n_p \leq N - 1\right)$ sub-carrier. Specifically, for any k_{th} block all the $\left(n_{(p-1)\Gamma+\mathrm{i}}, n_{(p-1)\Gamma+\mathrm{j}}\right)_{th}$ entries of $\varrho[(\boldsymbol{v} - \acute{\boldsymbol{v}})]\varrho[(\boldsymbol{v} - \acute{\boldsymbol{v}})]^H$ are non-zero, where $p = 1,2, \dots, P$ and $1 \leq i, j \leq \Gamma$. Thus all the $\left(n_{(p-1)\Gamma+\mathrm{i}}, n_{(p-1)\Gamma+\mathrm{j}}\right)_{th}$ entries of $(\varrho[(\boldsymbol{v} - \acute{\boldsymbol{v}})]\varrho[(\boldsymbol{v} - \acute{\boldsymbol{v}})]^H) \odot \boldsymbol{R}$ are non-zero. We define $\boldsymbol{T}_p, p = 1,2, \dots, P$ as the $\Gamma \times \Gamma$ matrix which determines the entries of

$(\varrho[(\boldsymbol{v}-\acute{\boldsymbol{v}})]\varrho[(\boldsymbol{v}-\acute{\boldsymbol{v}})]^H) \odot \boldsymbol{R}$. In other words, the $(i,j)_{th}$ entries of $\boldsymbol{T}_p$ (where $1 \le i,j \le \Gamma$) is the $\left(n_{(p-1)\Gamma+\mathrm{i}}, n_{(p-1)\Gamma+\mathrm{j}}\right)_{th}$ entry of $(\varrho[(\boldsymbol{v}-\acute{\boldsymbol{v}})]\varrho[(\boldsymbol{v}-\acute{\boldsymbol{v}})]^H) \odot \boldsymbol{R}$.

Using the derivations in Appendix C we can calculate the overall diversity product after interleaving as

$$\zeta_{eq} = \frac{1}{2}\min_{\acute{\mathbf{V}}_{k+1}\neq \mathbf{V}_{k+1}\forall \boldsymbol{v}} \left|\det\left(\acute{\boldsymbol{V}}^{k+1} - \boldsymbol{V}^{k+1}\right)\right|^{\frac{1}{P\Gamma}} . \left(\prod_{p=1}^{\mathrm{P}} \left|det\left(\boldsymbol{W}_p diag\left(\sigma_{(0)}^2, \dots, \sigma_{(L-1)}^2\right)\boldsymbol{W}_p^H\right)\right|\right)^{\frac{1}{2P\Gamma}}$$

$$= \zeta_c . \zeta_s \tag{28}$$

where $\boldsymbol{W}_p = \left[\boldsymbol{w}^{0^T}, \dots, \boldsymbol{w}^{(L-1)^T}\right]^T$, $\boldsymbol{w} = \left[1, \omega^1, \dots, \omega^{(PL-1)}\right]$. We observe from (28) above that ζ_s is only determined by the power delay profile and thus the interleaving approach can independently maximize ζ_s. On the other hand, ζ_c which was defined earlier is only dependent on the constellation design and code structure.

V. PERFORMANCE EVALUATION

In this section, we present simulation results to demonstrate the performance of our proposed differential DQSFC protocols. The settings for our cooperative broadband network are based on the specifications described in the IEEE802.16e Mobile WiMax standard. The number of sub-carriers used is $N = 200$ with a channel bandwidth of 3.5MHz. We assume that neither the relay nodes nor destination can acquire CSI. The frequency selective channels of the source-relay and relay-destination links remain approximately constant within two consecutive blocks, which is required for differential decoding as explained earlier. We illustrate the frequency diversity performance of our proposed differential DQSFC protocol using BPSK modulation. In our simulation, we observe that for scenarios where $L_{SR_1} \neq \cdots \neq L_{SR_p}$ and $L_{RD_1} \neq \cdots \neq L_{RD_p}$, the achievable diversity order is bounded by $min\left\{L_{SR_1}, \dots, L_{SR_p}\right\}$ and $min\left\{L_{RD_1}, \dots, L_{RD_p}\right\}$. This implies that the presence of additional fading paths on any of the source-relay or relay-destination links cannot provide additional diversity gain. Based on this, we only present results for the case of:

$L_{SR_1} = \cdots = L_{SR_p}$, $L_{RD_1} = \cdots = L_{RD_p}$, $L_{SR} = \{1, \dots, 4 \dots\}$,$L_{RD} = \{1, \dots, 4 \dots\}$

$\alpha_l = \beta_l \in \{0\mu s, 0.5\mu s, 1.5\mu s, 5\mu s\}$, $\sigma_{SR(1)} = \cdots = \sigma_{SR(L_{SR})} = 1$, $\sigma_{RD(1)} = \cdots = \sigma_{RD(L_{SR})} = 1$

For frequency diversity analysis, we consider two main scenarios; the symmetric case where $L_{SR} = L_{RD}$, and the asymmetric case where $L_{SR} \neq L_{RD}$. We consider the symmetric case in Fig.3, for $P = 4$ relay nodes, we first set $L = L_{SR} = L_{RD} = 2$ to form the basis for comparing our differential DQSFC scheme

with the non-differential DSFC scheme of [20] where $L = 2$ and $P = 4$. We consider SER performance to enable fair comparison with the scheme of [20]. From the results, we observe that the SER performance of our scheme slightly surpasses that of [20] despite the 3dB loss incurred by our scheme due to differential decoding. Our curve denoted 'Differential DQSFC $L = 2$ $P = 4$' also has a similar slope to that of [20]. This indicates that, like coherent designs, our non-coherent design exploits the maximum spatial and frequency diversity available in frequency selective channels even in scenarios where CSI cannot be acquired. In addition, while the scheme in [20] has full symbol rate, our scheme has the additional advantage of full code rate for $P \geq 2$ relays. We also observe that our scheme shows corresponding performance improvement when the number of channel taps increases from $L = 1$ (corresponding to a flat fading channel) to $L = 3$.

In Fig.4 we include the results for scenarios where $L_{SR} \neq L_{RD}$ to verify the achievable diversity gain based on our PEP analysis. From the results, we observe that the SER curve of our differential DQSFC scheme when $L_{SR} = 2$ and $L_{RD} = 3$ has the same slope as that of $L_{SR} = 3$ and $L_{RD} = 2$ which signifies that for cases where $L_{SR} \neq L_{RD}$ the diversity performance is bounded by $PL = P(min\{L_{SR}, L_{RD}\})$ which is consistent with the achievable diversity order based on our PEP analysis. Thus maximal diversity order is achieved when the coding at the source node and relay nodes are designed using $L = min\{L_{SR}, L_{RD}\}$. We also observe that a gain of about 1dB is achieved when L_{SR} exceeds L_{RD}. This implies that the extra channel taps on the source-relay link provides stronger error performance in comparison with the case when L_{RD} exceeds L_{SR}. This is owed to the fact that when L_{SR} exceeds L_{RD}, the relay nodes deliver less erroneous symbols to the destination. We then vary the number of channel taps using $L = 1$ and $L = 2$ for different number of relay nodes $P = 2$ and $P = 4$. We can observe from Fig.4 that for different cases, a diversity order of PL is achieved. For example, the differential DQSFC curve with $L = 1$ and $P = 4$ has an identical slope to that of $L = 2$ and $P = 2$. This confirms that our scheme exploits the achievable spatial and frequency diversity when quasi-orthogonal codes are utilized in scenarios where CSI is unavailable. In terms of SER performance, we can also deduce that the spatial diversity advantage (due to number of relays) slightly supersedes the multipath diversity advantage (due to number of channel taps).

In Fig.5 we analyse the diversity performance of our full rate quasi-orthogonal design using optimum rotation angles and sub-carrier interleaving, where $P = 4, L = 2$. For our quasi-orthogonal codes, the

optimum rotation angles are set as $\{1, \pi/M\}$, where $M = 2$ is the constellation size. To illustrate the diversity gain due to constellation rotation, we include the SER curve of non-rotated differential DQSFC schemes. We observe from Fig.5 that compared to our differential DQSFC scheme with optimum rotation angles, non-rotated differential DQSFC schemes exhibit similar performance at SNR values below 15dB. At higher SNR values, our differential DQSFC scheme with optimum rotation angles exhibits better performance. Simulation results also show that when interleaving is applied, there is a 1-2.5dB improvement compared to the case where interleaving is not applied. The curve for coherent DQSFC (where the effect of differential decoding parameters A and B is negligible) shows that a BER loss of about 1.5dB is incurred by our differential DQSFC scheme due to the noise impairing parameters. However, since the curve for coherent DQSFC has a similar slope to that of differential DQSFC, the loss in diversity performance is very small.

VI. CONCLUSIONS

The problem of designing full rate full diversity space-frequency codes for non-coherent cooperative broadband networks is addressed in this work. Apart from providing non coherent detection, our proposed DQSFC scheme offers a systematic design of quasi-orthogonal codes that can exploit the achievable spatial and frequency diversity available in frequency-selective fading cooperative networks. Through PEP analysis, we show that the diversity performance of our scheme can be improved by appropriate code construction and sub-carrier allocation. Based on this, we devise a code structure and sub-carrier allocation method to maximize the diversity performance of our scheme. Simulation results show that our proposed schemeexploits the maximum spatial and frequency diversity available in frequency selective channels even in scenarios where CSI cannot be acquired. The results also show that the availability of different number of paths on the source-relay and relay-destination links provides additional diversity gains. We note from simulation results that although the non-coherent detection algorithm employed by our scheme incurs slight degradation in error performance, the achievable diversity gain is sufficiently preserved.

APPENDIX A

In this appendix, we show that the performance of our quasi-orthogonal code is determined by $\boldsymbol{R}$, $\boldsymbol{\Lambda}^H\boldsymbol{\Lambda}$ and $\left(\acute{\boldsymbol{V}}^{k+1}-\boldsymbol{V}^{k+1}\right)^H\left(\acute{\boldsymbol{V}}^{k+1}-\boldsymbol{V}^{k+1}\right)$. The consecutively received signals at the destination in (26) can be written in matrix form as:

$$\boldsymbol{Y}=\boldsymbol{X}\mathbf{W}\boldsymbol{h}+\boldsymbol{Z} \tag{29}$$

The conditional probability density function of the receive signal matrix $\boldsymbol{Y}$ is

$$p\left(\boldsymbol{Y}\middle|\boldsymbol{V}^{k+1}\right)=\frac{\exp(-tr\{\boldsymbol{Y}(\boldsymbol{I}_{P\Gamma}+\Upsilon\boldsymbol{X}\boldsymbol{\Lambda}\boldsymbol{R}\boldsymbol{\Lambda}^H\boldsymbol{X}^H)^{-1}\boldsymbol{Y}^H\})}{\pi^{P\Gamma}\det(\boldsymbol{I}_{P\Gamma}+\Upsilon\boldsymbol{X}\boldsymbol{\Lambda}\boldsymbol{R}\boldsymbol{\Lambda}^H\boldsymbol{X}^H)} \tag{30}$$

where $\mathbf{C}_{\mathrm{v}}=(\boldsymbol{I}_{P\Gamma}+\Upsilon\boldsymbol{X}\boldsymbol{\Lambda}\boldsymbol{R}\boldsymbol{\Lambda}^H\boldsymbol{X}^H)$ is the covariance matrix of $\boldsymbol{Y}$, tr denotes the trace function and Υ is the average SNR of the received signal given as $\Upsilon=\frac{P\Upsilon_{SR}\Upsilon_{RD}}{1+\Upsilon_{SR}+P\Upsilon_{RD}}$. Thus the non-coherent ML decoder is given by:

$$\widehat{\boldsymbol{V}}^{k+1}=\arg\max_{\boldsymbol{V}^{k+1}\in\boldsymbol{\mathcal{V}}}p\left(\boldsymbol{Y}\middle|\boldsymbol{V}^{k+1}\right) \tag{31}$$

Substituting $\boldsymbol{Y}^k$into $\boldsymbol{Y}^{k+1}$in (26) and using $\overline{\boldsymbol{X}}^{k+1}=\boldsymbol{V}^{k+1}\overline{\boldsymbol{X}}^k$ we have $\boldsymbol{Y}^{k+1}=\boldsymbol{V}^{k+1}\boldsymbol{Y}^k+\grave{\boldsymbol{Z}}^{k+1}$ where$\grave{\boldsymbol{Z}}^{k+1}=\boldsymbol{Z}^{k+1}-\boldsymbol{V}^{k+1}\boldsymbol{Z}^k$. The non-coherent ML decoder can thus be simplified as

$$\widehat{\boldsymbol{V}}^{k+1}=\arg\max_{\boldsymbol{V}^{k+1}\in\boldsymbol{\mathcal{V}}}\left\|\boldsymbol{Y}^k+\boldsymbol{V}^{k+1^H}\boldsymbol{Y}^{k+1}\right\| \tag{32}$$

where $\|\cdot\|$ is the Frobenius norm. The Chernoff bound on the PEP of mistaking $\boldsymbol{V}^{k+1}$ by $\acute{\boldsymbol{V}}^{k+1}$ can be given as [18] [19].

$$PEP\left(\boldsymbol{V}^{k+1}-\acute{\boldsymbol{V}}^{k+1}\right)=\frac{1}{2}\left\{\frac{\det\left[\lambda(\boldsymbol{I}_{P\Gamma}+\Upsilon\boldsymbol{X}\boldsymbol{\Lambda}\boldsymbol{R}\boldsymbol{\Lambda}^H\boldsymbol{X}^H)+(1-\lambda)\left(\boldsymbol{I}_{P\Gamma}+\Upsilon\acute{\boldsymbol{X}}\boldsymbol{\Lambda}\boldsymbol{R}\boldsymbol{\Lambda}^H\acute{\boldsymbol{X}}^{\boldsymbol{H}}\right)\right]}{\det^{\lambda}(\boldsymbol{I}_{P\Gamma}+\Upsilon\boldsymbol{X}\boldsymbol{\Lambda}\boldsymbol{R}\boldsymbol{\Lambda}^H\boldsymbol{X}^H)\cdot\det^{(1-\lambda)}\left(\boldsymbol{I}_{P\Gamma}+\Upsilon\acute{\boldsymbol{X}}\boldsymbol{\Lambda}\boldsymbol{R}\boldsymbol{\Lambda}^H\acute{\boldsymbol{X}}^{\boldsymbol{H}}\right)}\right\} \tag{33}$$

where $\boldsymbol{X}$ and $\acute{\boldsymbol{X}}$ are two distinct codewords, $\acute{\boldsymbol{X}}=\left[\boldsymbol{I}_{P\Gamma}{}^T,\acute{\boldsymbol{V}}^{k+1^T}\right]$ and $\lambda=E\{\exp(\lambda[\ln p\left(\boldsymbol{Y}\middle|\boldsymbol{V}^{k+1}\right)-p\left(\boldsymbol{Y}\middle|\acute{\boldsymbol{V}}^{k+1}\right)])\}$ is used to get the tightest bound. By simple algebraic manipulation (33) can be simplified as

$$PEP\left(\boldsymbol{V}^{k+1}-\acute{\boldsymbol{V}}^{k+1}\right)=\frac{1}{2}\left\{\frac{\det\left[\boldsymbol{I}_{P\Gamma}+\Upsilon\boldsymbol{\Lambda}\boldsymbol{R}\boldsymbol{\Lambda}^H\left(\boldsymbol{X}\lambda\boldsymbol{X}^{\boldsymbol{H}}+\acute{\boldsymbol{X}}(1-\lambda)\acute{\boldsymbol{X}}^{\boldsymbol{H}}\right)\right]}{\det[\boldsymbol{I}_{P\Gamma}+2\Upsilon\boldsymbol{\Lambda}\boldsymbol{R}\boldsymbol{\Lambda}^H]}\right\} \tag{34}$$

Since the relay nodes in our scheme linearly process their received signals, our achievable diversity order is bounded by $L=min\{L_{SR},L_{RD}\}$. Thus, targeting maximum diversity order we choose $\Gamma=L$. Other values of Γ may be desirable, for example, when targeting minimum decoding complexity or when high

SNR is considered. We can deduce from (34) that for all values of k, if $\acute{\boldsymbol{V}}^{k+1} - \boldsymbol{V}^{k+1}$ or similarly if $\acute{\boldsymbol{X}} - \boldsymbol{X}$ has full rank, then our scheme will achieve a diversity order of PL. At high SNR, the term in (34) can be further bounded as (35) where $\lambda = 1/2$ is selected to get the tightest bound [18].

$$PEP\left(\boldsymbol{V}^{k+1} - \acute{\boldsymbol{V}}^{k+1}\right) \leq \left(\frac{\gamma}{8}\left(\det(\boldsymbol{\Lambda R \Lambda}^H)\det\left[\left(\acute{\boldsymbol{V}}^{k+1} - \boldsymbol{V}^{k+1}\right)^H\left(\acute{\boldsymbol{V}}^{k+1} - \boldsymbol{V}^{k+1}\right)\right]\right)^{\frac{1}{PL}}\right)^{-PL} \quad (35)$$

APPENDIX B

In this appendix, we prove that our quasi-orthogonal code satisfies the full diversity criterion for space-frequency codes.

Proof: Given two distinct pair of codewords $\boldsymbol{\mathcal{V}}_k = diag[\mathcal{G}(v_1, v_2), \dots, \mathcal{G}(v_{P\Gamma-1}, v_{P\Gamma})]$ and $\acute{\boldsymbol{\mathcal{V}}}_k = diag[\mathcal{G}(\acute{v}_1, \acute{v}_2), \dots, \mathcal{G}(v_{P\acute{\Gamma}-1}, v'_{P\Gamma})]$, the coding gain difference (CGD) is given by [14, Section 5.2].

$$det\left[\left(\boldsymbol{\mathcal{V}}_k - \acute{\boldsymbol{\mathcal{V}}}_k\right)^H\left(\boldsymbol{\mathcal{V}}_k - \acute{\boldsymbol{\mathcal{V}}}_k\right)\right] = P\Gamma det\left[\left(\mathcal{G}(v_1, v_2) - \mathcal{G}(\acute{v}_1, \acute{v}_2)\right)\right]det\left[\left(\mathcal{G}(v_3, v_4) - \mathcal{G}(\acute{v}_3, \acute{v}_4)\right)\right]\dots$$

$$det\left[\left(\mathcal{G}(v_{P\Gamma-1}, v_{P\Gamma}) - \mathcal{G}(v_{P\acute{\Gamma}-1}, v'_{P\Gamma})\right)\right] \quad (36)$$

$$= (|v_1 - \acute{v}_1|^2 + |v_2 - \acute{v}_2|^2)^2(|v_3 - \acute{v}_3|^2 + |v_4 - \acute{v}_4|^2)^2 \dots (|v_{P\Gamma-1} - v_{P\acute{\Gamma}-1}|^2 + |v_{P\Gamma} - v'_{P\Gamma}|^2)^2 \quad (37)$$

where $\acute{v}_1 = \acute{\mathrm{v}}_1 + \acute{\tilde{\mathrm{v}}}_3 + \cdots$, $\acute{v}_2 = \acute{\mathrm{v}}_2 + \acute{\tilde{\mathrm{v}}}_4 + \cdots$, $\acute{v}_3 = \acute{\mathrm{v}}_1 - \acute{\tilde{\mathrm{v}}}_3 - \cdots$, $\acute{v}_4 = \acute{\mathrm{v}}_2 - \acute{\tilde{\mathrm{v}}}_4 - \cdots$ and so on. The bit label $\acute{\tilde{\mathrm{v}}}_\iota$ is the rotated version of $\acute{\mathrm{v}}_\iota$ by θ. In order to guarantee that the code achieves full diversity, the rotation angles $\{\theta_1, \theta_2, \dots, \theta_{P\Gamma}\}$ corresponding to $\{\mathrm{v}_1, \mathrm{v}_2, \dots, \mathrm{v}_{P\Gamma}\}$ and $\{\acute{\mathrm{v}}_1, \acute{\mathrm{v}}_2, \dots, \acute{\mathrm{v}}_{P\Gamma}\}$ are selected such that $det\left[\left(\mathcal{G}(v_i, v_j) - \mathcal{G}(\acute{v}_\iota, \acute{v}_j)\right)\right] \neq 0, \forall\, i, j \in \{1,2, \dots, P\Gamma\}$. This equivalently means that $(\mathrm{v}_i - \acute{\mathrm{v}}_\iota) + (\mathrm{v}_j - \acute{\mathrm{v}}_j) \neq 0, \forall\, i, j \in \{1,2, \dots, P\Gamma\}$. Therefore we can deduce from (37) that $\prod_{p=1}^{P\Gamma}|v_p - \acute{v}_p|^2 \neq 0$.

APPENDIX C

Given that the correlation matrix $\boldsymbol{R} = \boldsymbol{R}_1 \odot \boldsymbol{R}_2$, and $\boldsymbol{R}$, $\boldsymbol{R}_1$ and $\boldsymbol{R}_2$ have the structure of a Toeplitz matrix, the correlation co-efficient between the $(i,j)_{th}(0 \leq i, j \leq N-1)$entries of $\boldsymbol{R}_1$ and $\boldsymbol{R}_2$ are given respectively as $R_{1i,j} = \sum_{l=0}^{L_{SR}-1} {\sigma_{SR}}_l^2\, \omega^{(i-j)\alpha_l}$ and $R_{2i,j} = \sum_{l=0}^{L_{RD}-1} {\sigma_{RD}}_l^2\, \omega^{(i-j)\beta_l}$. From this we obtain the correlation co-efficient between the $(i,j)_{th}(0 \leq i, j \leq N-1)$ entries of $\boldsymbol{R}$ as

$$R_{i,j} = \sum_{l=0}^{L-1} \sigma_l^2\, \omega^{(i-j)\tau_l} \quad (38)$$

where $\sigma_l^2 = {\sigma_{SR}}_l^2 \cdot {\sigma_{RD}}_l^2$ and $\tau_l = min(\alpha_l, \beta_l)$. Thus the correlation co-efficient between the $(i,j)_{th}(1 \leq i, j \leq \Gamma)$ entries of $\boldsymbol{T}_p$ can be given by

$$T_{pi,j} = \Delta \sum_{l=0}^{L-1} \sigma_l^2\, \omega^{\left(n_{(p-1)\Gamma+\mathrm{i}}, n_{(p-1)\Gamma+\mathrm{j}}\right)\tau_l} \quad (39)$$

where $\Delta = P.[(v_c - \acute{v_c})(v_d - \acute{v_d})^*],\ c = (p-1)\Gamma + i,$ and $d = (p-1)\Gamma + j.$ The $\Gamma \times \Gamma$ matrix $\boldsymbol{T}_p, p = 1, \dots, P$ can be represented by

$$\boldsymbol{T}_p = \bar{\Delta}\boldsymbol{W}_p diag\left(\sigma^2_{(0)}, \dots, \sigma^2_{(L-1)}\right)\boldsymbol{W}_p^H \bar{\Delta}^H \tag{40}$$

where $\bar{\Delta} = \sqrt{P}.[(v_c - \acute{v_c})(v_d - \acute{v_d})^*]$ and $\boldsymbol{W}_p = \left[\boldsymbol{w}^{0^T}, \dots, \boldsymbol{w}^{(L-1)^T}\right]^T$, $\boldsymbol{w} = \left[1, \omega^1, \dots, \omega^{(PL-1)}\right]$

We can calculate the determinant of $\boldsymbol{T}_p$ as

$$det\left(\boldsymbol{T}_p\right) = P^{\Gamma} \prod_{i=1}^{\Gamma} |(v_c - \acute{v_c})|^2 \, det\left(\boldsymbol{W}_p diag\left(\sigma^2_{(0)}, \dots, \sigma^2_{(L-1)}\right)\boldsymbol{W}_p^H\right) \tag{41}$$

Thus the overall diversity product after interleaving is

$$\zeta_{eq} = \frac{1}{2}\min_{\acute{\boldsymbol{v}}_k \neq \boldsymbol{v}_k \forall \boldsymbol{v}} \left(\prod_{p=1}^{P\Gamma} |(v_c - \acute{v_c})|\right)^{\frac{1}{P\Gamma}} \left(\prod_{p=1}^{P} \left|det\left(\boldsymbol{W}_p diag\left(\sigma^2_{(0)}, \dots, \sigma^2_{(L-1)}\right)\boldsymbol{W}_p^H\right)\right|\right)^{\frac{1}{2P\Gamma}}$$

$$= \frac{1}{2}\min_{\acute{\mathbf{v}}_{k+1} \neq \mathbf{v}_{k+1} \forall \boldsymbol{v}} \left|\det\left(\acute{\boldsymbol{V}}^{k+1} - \boldsymbol{V}^{k+1}\right)\right|^{\frac{1}{P\Gamma}} . \left(\prod_{p=1}^{P} \left|det\left(\boldsymbol{W}_p diag\left(\sigma^2_{(0)}, \dots, \sigma^2_{(L-1)}\right)\boldsymbol{W}_p^H\right)\right|\right)^{\frac{1}{2P\Gamma}}$$

$$= \zeta_c . \zeta_s \tag{42}$$

REFERENCES

[1] E.Baccarelli,M.Biagi,C.Pelizzoni,N. Cordeschi, "Optimal MIMO UWB-IR transceiver for Nakagami-fading and Poisson-arrivals", Journal of Communication,vol.3,no.1, pp. 27-40, Jan. 2008.

[2] E.Baccarelli,M. Biagi, "A novel self-pilot-based transmit-receive architecture for multipath impaired UWB systems", IEEE Transactions on Communications, vol.52,no.6,pp. 891-895, Jun. 2004.

[3] Y. Jing and H. Jafarkhani, "Distributed differential space-time coding for wireless relay networks," IEEE Transactions on Communications, vol. 56, no. 7, pp. 1092-1100, Jul. 2008.

[4] G. Susinder Rajan, and B. Sundar Rajan, "Algebraic distributed differential space-time codes with low decoding complexity," IEEE Transactions on Wireless Communications, vol. 7, no. 10, pp. 3962-3971, 2008.

[5] S. Sugiura, Sheng Chen,H. Haas, P.M. Grant, L. Hanzo, "Coherent versus non-coherent decode-and-Forward Relaying Aided Cooperative Space-Time Shift Keying," IEEE Transactions on Communications, vol. 59, no. 6, pp. 1707-1719, 2011.

[6] W. Su and X. Xia, "Signal constellations for quasi-orthogonal space time block codes with full diversity," IEEE Transactions on Information Theory, vol. 50, no. 10, pp. 2331-2347, Oct. 2004.

[7] Y. Jing, and H. Jafarkhani, "Using orthogonal and quasi-orthogonal designs in wireless relay networks," IEEE Transactions on Information Theory, vol. 53, no. 11, pp. 4106-4118, Nov. 2007.

[8] F. Fazel and H. Jafarkhani, "Quasi-orthogonal space-frequency and space-time-frequency block codes for MIMO OFDM channels," IEEE Transactions on Wireless Communications, vol. 7, no. 1, pp. 184-192, Jan. 2008.

[9] H. Zhang, D. Yuan, and H. Chen, "On Array-Processing-Based Quasi-Orthogonal Space–Time Block-Coded OFDM Systems," IEEE Transactions on Vehicular Technology, vol. 59, no.1, pp. 508-513, Jan. 2010.

[10] W. Su and K.J. Ray Liu, "Full-rate full-diversity space-frequency codes with optimum coding advantage" IEEE Transactions on Information Theory, vol. 51, no. 1, pp. 229-249, Jan. 2005.

[11] X. Li, Y. Wu, and E. Serpedin, "Timing synchronization in decode-and-forward cooperative communication systems," IEEE Transactions on Signal Processing, vol. 57, no. 4, pp. 1444-1455, April 2009.

[12] J. G. Andrews, A. Ghosh, R. Muhamed, Fundamentals ofWiMAX: Understanding Broadband wireless Networking, Prentice Hall, 2007.

[13] H. X. Nguyen and H. H. Nguyen, "Adaptive relaying in non-coherent cooperative networks,"IEEE Transactions on Signal Processing, vol. 58, no. 7, pp. 3938-3945, July 2010.
[14] H. Jafarkhani, Space-time Coding Theory and Practice, Chapter 5, Cambridge Academic Press, 2005.
[15] W. Su, Z. Safar, and K. J. Ray Liu, "Towards maximum achievable diversity in space, time, and frequency: performance analysis and code design," IEEE Transactions on Wireless Communications, vol. 4, no. 4, pp. 1847-1857, July 2005.
[16] Z. Liu, Y. Xin, and G. B. Giannakis, "Linear constellation precoding for OFDM with maximum multipath diversity and coding gains," IEEE Transactions on Communications, vol. 51, no. 3, pp. 416-427, March 2003.
[17] R. Bhatia, Positive Definite Matrices, Princeton Series in Applied Mathematics, 2007.
[18] Q. Ma, C. Tepedelenlioglu, and Z. Liu, "Differential space-time-frequency coded OFDM with maximum multipath diversity," IEEE Transactions on Wireless Communications, vol. 4, no. 5, pp. 2232–2243, 2005.
[19] A. Dogandzic, "Chernoff bounds on pairwise error probabilities of space–time codes," IEEE Transactions on Information Theory, vol. 49, no. 5, pp. 1327–1336, May 2003.
[20] W. Zhang, Y. Li, X. Xia, P.C. Ching, and K.B. Letaief, "Distributed space-frequency coding for cooperative diversity in broadband wireless Adhoc networks," IEEE Transactions on Wireless Communications, vol. 7, no. 3, pp. 995-1003, Mar. 2008.

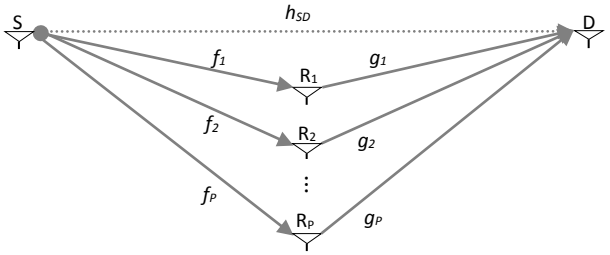

Fig.1 P-relay Cooperative Network

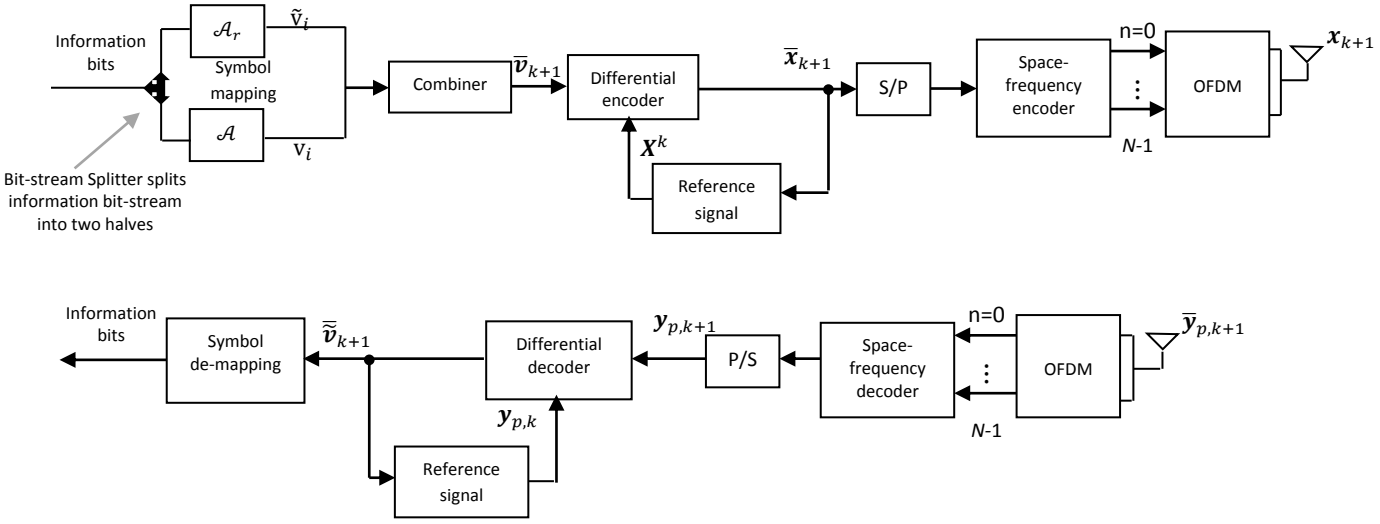

Fig.2. Differential DQSFC System Architecture

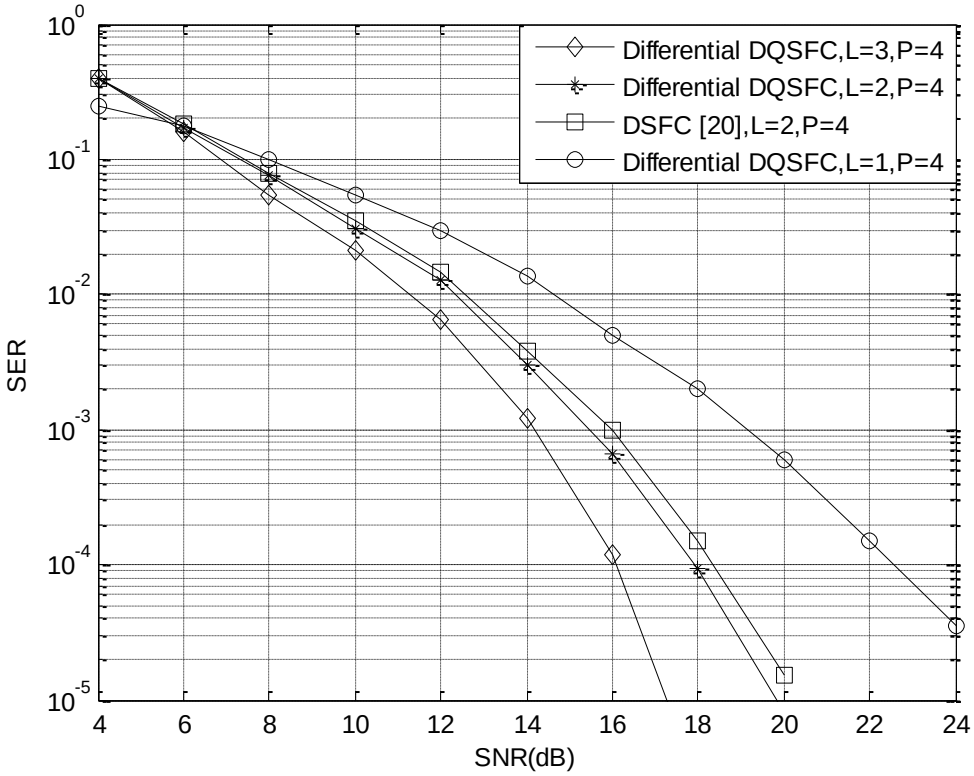

Fig.3 Frequency diversity performance of differential DQSFC scheme for the symmetric case

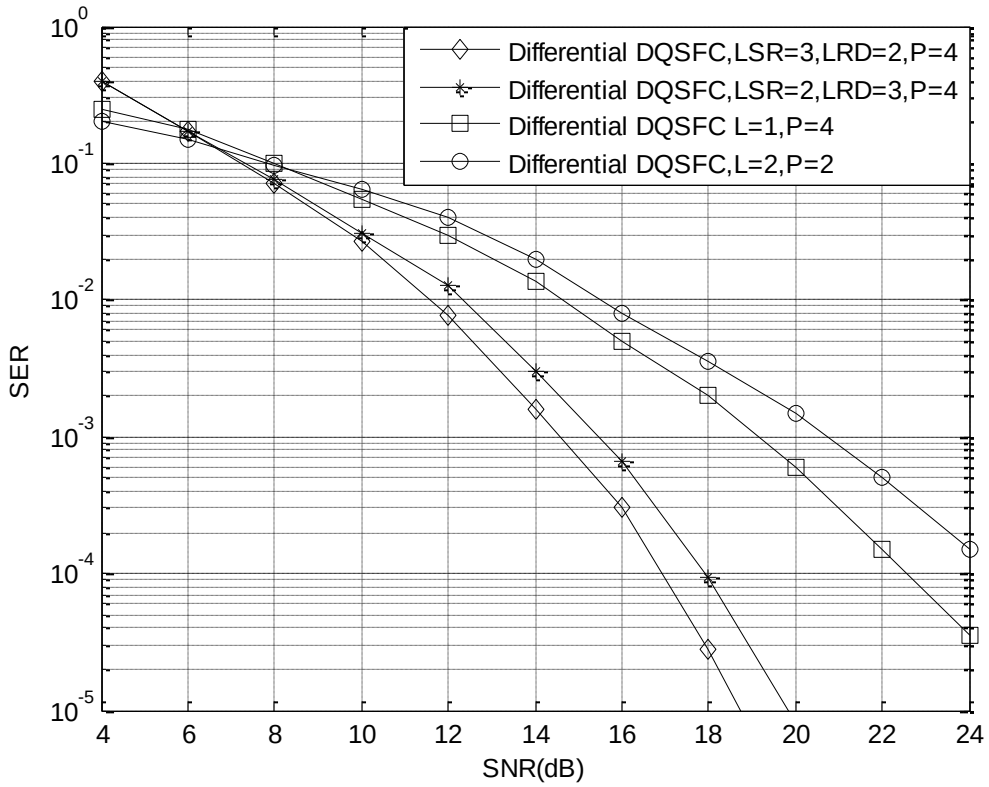

Fig.4 Frequency diversity performance of differential DQSFC scheme for the asymmetric case

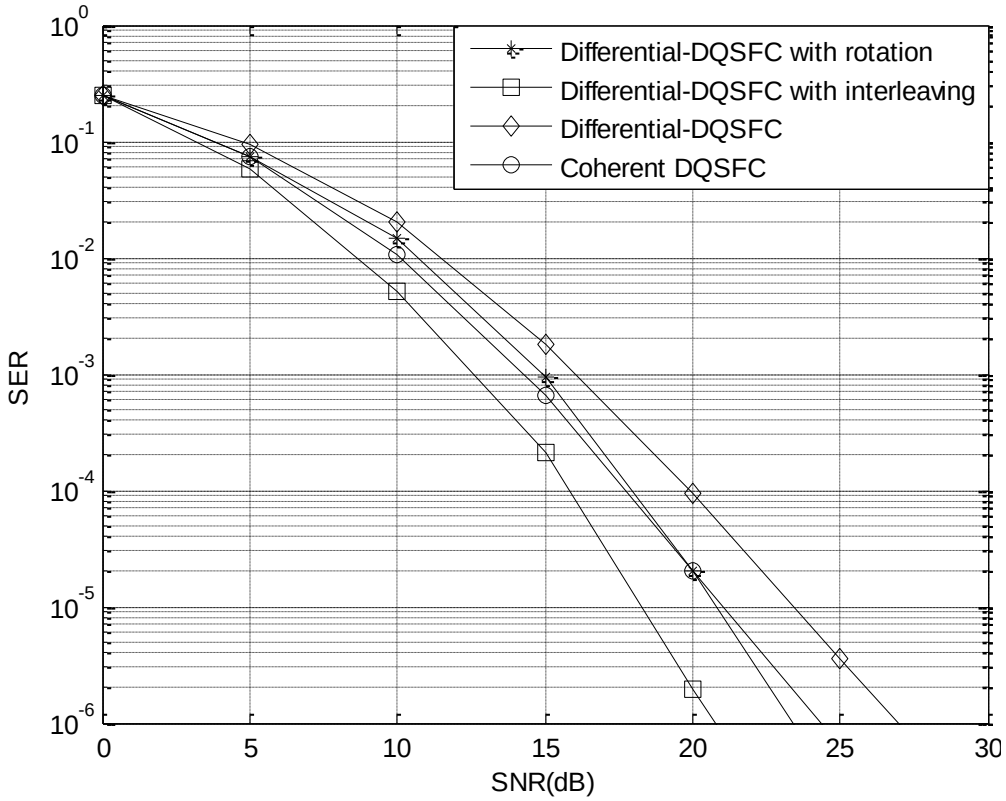

Fig.5 Diversity performance of differential DQSFC scheme with optimum constellation rotation and interleaving